JOURNAL OF SOLID STATE CHEMISTRY 53, 406–414 (1984)

Luminescent Properties of Nd^{3+} in the $Na_xNd_xM_{(1-2x)}Ga_2S_4$ Thiogallates (M = Ca,Sr,Ba; $x \leq 0.5$): A Family of Materials Characterized by Weak Self-Quenching and Efficient Band Excitation

R. IBAÑEZ,* A. GARCIA, C. FOUASSIER, AND P. HAGENMULLER

Laboratoire de Chimie du Solide du CNRS, Université de Bordeaux I 351, cours de la Libération, 33405 Talence Cedex, France

Received November 22, 1983

As a consequence of the weak phonon energies and the low crystal field, several excited states of Nd^{3+} are emitters in the $Na_xNd_xM_{1-2x}Ga_2S_4$ thiogallates ($x \leq 0.5$ for M = Ca or Sr and ≤ 0.2 for M = Ba). The infrared $^4F_{3/2}$ emission is little affected by concentration quenching. $NaNdGa_4S_8$ is the first efficient stoichiometric sulfide so far reported. Unlike other sulfides previously investigated, the neodymium thiogallates show an intense excitation band, ascribed to electron transfer from the valence band to states constituted essentially by neodymium orbitals.

Introduction

The chalcogenides are attractive host lattices for rare-earth ions, as the probability of the parity-forbidden f–f transitions is increased by the covalency of the bonding, while nonradiative processes are reduced owing to the weak energy of phonons. Neodymium-doped sulfides could be of interest for laser application:

(i) For host lattices in which the rare-earth sites are isolated, a weak self-quenching of the $^4F_{3/2}$ emission is expected from the low intensity of the ligand field. Crystals combining high neodymium concentration and large f–f oscillator strengths would be characterized by a very low pumping threshold when excited by a visible radiation.

(ii) Sulfides are potential materials for rare-earth semiconductor lasers. Neodymium can be incorporated into ZnS and CdS (*1*); the doped samples show photo- and electroluminescent properties (*2–4*) and evidence for stimulated emission has been recently shown (*5*). Only small rare-earth amounts can be accommodated by the network of the II–VI semiconductors. This is not the case when neodymium is substituted for another rare-earth. Recently the luminescence of neodymium in Ln_2S_3 crystals (Ln = La,Gd,Y) (*6, 7, 26*) and La_2S_3–M_2S_3 glasses (M = Al,Ga) (*8, 9*) has been investigated.

A major drawback of rare-earth sulfides is the large number of lattice defects, which is a consequence of the weakness of the bonding. This results in particular in a very poor efficiency of the excitation in the host lattice since defects compete with rare-earth ions for the capture of charge carriers or excitons.

* Permanent address: Departamento de Química Inorgánica, Facultad de Ciencias Químicas, Universidad de Valencia, Av. Dr. Moliner s/n Burjasot, Valencia, España.

0022-4596/84 $3.00

In the MGa_2S_4 thiogallates (M = Ca,Sr, Ba) the alkaline earth can be substituted by a trivalent rare-earth with charge compensation by sodium ions (*10, 11*). The strength of the covalent Ga–S bonds is increased by the presence of the alkali and alkaline earth elements, so that a reduction of the tendency to defect formation can be inferred. The present paper describes the luminescent properties of neodymium in this family of compounds.

I. Syntheses and Structural Investigation

The $Na_xNd_xM_{1-2x}Ga_2S_4$ phases have been obtained from mixtures of $NaNdS_2$, Ga_2S_3, and MGa_2S_4 (M = Ca, Sr, Ba) in a stream of H_2S gas:

$$x\mathrm{NaNdS_2} + 2x\mathrm{Ga_2S_3} + (1 - 2x)M\mathrm{Ga_2S_4} \rightarrow \mathrm{Na}_x\mathrm{Nd}_xM_{1-2x}\mathrm{Ga_2S_4}.$$

The sulfides $NaNdS_2$, Ga_2S_3, and MGa_2S_4 were prepared from Nd_2O_3 (Rhône-Poulenc, 99.99%), Ga_2O_3 (Touzart et Matignon, 99.999%), Na_2CO_3, and MCO_3 (Carlo-Erba). The mixed thiogallates could be obtained at 900°C for the low neodymium concentrations, at 800°C for the high concentrations. Higher preparation temperatures cause a decrease in the luminescence efficiency as a result of the formation of defects.

The $CaGa_2S_4$ and $SrGa_2S_4$ phases crystallize in the orthorhombic system, with space group *Fddd*, and are isostructural with Eu Ga_2S_4 (*10, 12*), whose structure has been recently determined (*13*). The divalent cations occupy three square antiprismatic sites. The alkaline earth can be entirely substituted by the neodymium and sodium ions. To get single crystals of the upper limit composition, $NaNdGa_4S_8$, a powder sample placed in a carbon crucible inside a sealed tube was maintained a few hours at 1100°C. Weissenberg photographs showed the systematic absences: hkl: $h + k$, $k + l = 2n + 1$, $0kl$: $k + l = 4n + 2$, $hk0$: $h + k = 4n + 2$, ($h00$: $h = 4n + 2$, $0k0$: $k = 4n + 2$) consistent with the space group *Fddd*. The cell dimensions were refined from powder data: $a = 20.18 \pm 0.01$ Å, $b = 20.18 \pm 0.01$ Å, $c = 12.15 \pm 0.01$ Å. The existence of a complete solid solution between $CaGa_2S_4$ and $Na_{0.5}Nd_{0.5}Ga_2S_4$ was checked.

The structure of the barium phase has just been determined (*14*). $BaGa_2S_4$ crystallizes in the cubic system, space group $Pa3$. The alkaline earth ions lie in two types of sites: of the 12 Ba^{2+} ions in the unit cell, 4 are in distorted octahedra, while 8 are 12-coordinated with much longer Ba–S distances. At 850°C the limit of substitution of Ba^{2+} ions corresponds to $x \simeq 0.20$. Under our preparation conditions the unit cell shows a distortion which disappears for $x = 0.03$. For the $Na_{0.04}Nd_{0.04}Ba_{0.92}Ga_2S_4$ composition, single crystals were grown by slow cooling from 1080°C. Diffraction photographs showed the systematic absences: $hk0$: $h = 2n + 1$, $0kl$: $k = 2n + 1$, $h0l$: $l = 2n + 1$, consistent with the space group $Pa3$.

II. Luminescent Properties

II-1. Experimental

Excitation and emission spectra were corrected for variation of the lamp flux and detector response, respectively. A dye laser pumped by a 6-nsec-pulsed nitrogen laser was used for determination of the fluorescent lifetimes. The signal was fed into a boxcar averager (PAR Model 162).

II-2. Emission Spectra

At low neodymium concentration the emission of several levels can be detected. The infrared $^4F_{3/2}$ emission is by far the most intense. In the visible the strongest lines are issued from the $^4G_{7/2}$ state; the mixture of the $^4G_{7/2} \rightarrow {}^4I_{9/2}$ ($\lambda \simeq 540$ nm) and $^4G_{7/2} \rightarrow {}^4I_{11/2}$ ($\lambda \simeq 600$ nm) transitions yields a yellow color. The $^4F_{3/2}$ and $^4G_{7/2}$ emissions

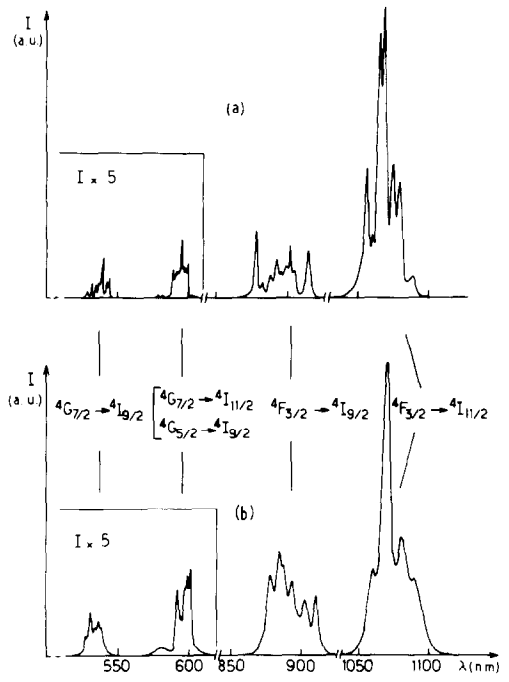

FIG. 1. $^4G_{7/2}$ and $^4F_{3/2}$ emissions for $Na_{0.01}Nd_{0.01}Ca_{0.98}Ga_2S_4$ (a) and $Na_{0.01}Nd_{0.01}Ba_{0.98}Ga_2S_4$ (b) at 300 K (λ_{exc} = 315 nm).

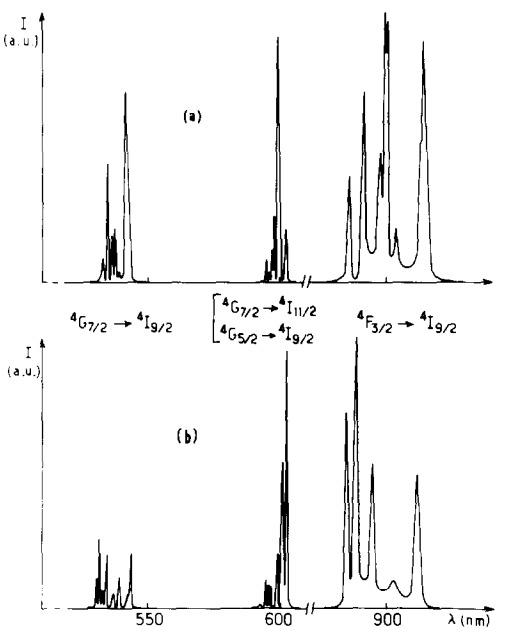

FIG. 2. $^4G_{7/2}$ and $^4F_{3/2}$ emissions for $Na_{0.01}Nd_{0.01}Ca_{0.98}Ga_2S_4$ (a) and $Na_{0.01}Nd_{0.01}Ba_{0.98}Ga_2S_4$ (b) at 4.2 K (intensities for the visible and ir range are not comparable).

for the $Na_{0.01}Nd_{0.01}Ca_{0.98}Ga_2S_4$ and $Na_{0.01}Nd_{0.01}Ba_{0.98}Ga_2S_4$ compositions at 300 and 4 K are shown in Figs. 1 and 2; the $^2P_{1/2}$ emission at 300 K is represented in Fig. 3. The neodymium emission in the strontium thiogallate shows strong similarities to that of the isomorphous calcium phase.

For $x < 0.5$ the local distortions resulting from the size differences between the Nd^{3+}, Na^+, and M^{2+} ions induce a broadening of the emission lines. The structural investigation of $EuGa_2S_4$ has shown that the divalent cations occupy three slightly different antiprismatic sites. In the emission spectrum of the $Na_xNd_xCa_{1-2x}Ga_2S_4$ phase, isostructural with $EuGa_2S_4$, a small splitting has been detected for some lines at low temperature, indicating a distribution of Nd^{3+} ions in two sites. For $x = 0.5$ most emission lines split into two narrower lines with similar intensities. It can be concluded that the Nd^{3+} ions are then equally distributed in an ordered way into two somewhat different types of sites. It is likely they occupy the *a* and *b* positions (8 sites per unit cell for every one), while the Na^+ ions lie in the (16*e*) sites. The coordination polyhedra associated with the *a* and *b* sites do not share apices, so repulsions between Nd^{3+} ions are

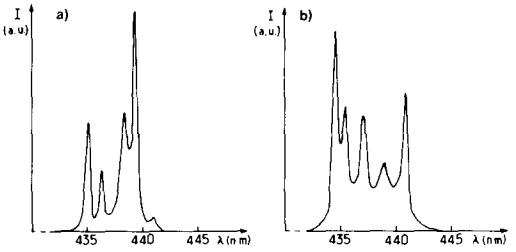

FIG. 3. $^2P_{1/2} \rightarrow {}^4I_{9/2}$ emission for $Na_{0.01}Nd_{0.01}Ca_{0.98}Ga_2S_4$ (a) and $Na_{0.01}Nd_{0.01}Ba_{0.98}Ga_2S_4$ (b) at 300 K (λ_{exc} = 315 nm).

minimized. Full determination of the structure will permit a check of this distribution.

In $BaGa_2S_4$, the divalent cations lie in two crystallographic positions, but all the emitting neodymium ions occupy the same type of sites. The linewidths, comparable to those of the calcium phase, are much narrower than those of the phonon-assisted transitions observed when Nd^{3+} is in a centrosymmetric position. So the emission is probably due to neodymium ions situated in the distorted noncentered octahedral sites.

The splittings of the J levels are small. The Stark components of the ground state are listed in Table I for the $Na_{0.01}Nd_{0.01}Ca_{0.98}Ga_2S_4$ and $Na_{0.01}Nd_{0.01}Ba_{0.98}Ga_2S_4$ compositions. As shown by Auzel (*15*), the splitting of the $^4I_{9/2}$ level provides an estimate of the intensity of the crystal field. The values observed for the thiogallates (328 and 322 cm^{-1}) are close to those of the low-crystal-field materials like NdP_5O_{14} (320 cm^{-1}) (*16*) and $LiNdP_4O_{12}$ (326 cm^{-1}) (*17*).

In oxides all the levels above $^4F_{3/2}$ are depopulated by multiphonon processes (for $^4G_{7/2}$ the energy gap with the next lower level is only about 1200 cm^{-1}). The existence of radiative transitions in the case of thiogallates is made possible by the weak energy of the phonons and the small splitting of the J levels.

II-3. Concentration Quenching

The emission issued from $^4G_{7/2}$ is strongly affected by concentration quenching. The overlapping of the $^4G_{7/2} \rightarrow {}^4I_{11/2}$ transitions with the intense $^4I_{9/2} \rightarrow {}^4G_{5/2}, {}^2G_{7/2}$ absorption lines (Figs. 1 and 7) leads to deexcitation by cross-relaxation. Moreover energy diffusion among Nd^{3+} ions can also occur at low concentration, the $^4I_{9/2} \rightarrow {}^4G_{7/2}$ transitions having high oscillator strengths. The initial portion of the decay, which deviates from exponentiality, corresponds to nonradiative losses by direct interactions (*18*). The final exponential portion characterized by a decay constant which decreases with increasing neodymium content indicates diffusion-limited relaxation. All the radiative transitions originating from other levels above $^4F_{3/2}$ are likewise rapidly quenched as x increases.

TABLE I

ENERGY OF THE STARK COMPONENTS OF THE $^4I_{9/2}$ LEVEL IN THE CALCIUM AND BARIUM THIOGALLATES AT 4 K (cm^{-1})

$Na_{0.01}Nd_{0.01}Ca_{0.98}Ga_2S_4$	$Na_{0.01}Nd_{0.01}Ba_{0.98}Ga_2S_4$
328	322
208	193
164	113
62	40
0	0

Concentration quenching of the $^4F_{3/2}$ emission is much less pronounced, as shown by the variation of the quantum efficiency for excitation into f–f lines (λ_{exc} = 594 nm) (Fig. 4) and by the slow decrease of fluorescent lifetimes (Fig. 5). As expected, Nd^{3+} shows a longer lifetime when incorporated into the distorted octahedra of the $BaGa_2S_4$ host lattice than in the antiprismatic sites of $CaGa_2S_4$, as the decay rate depends on the deviation from local inversion sym-

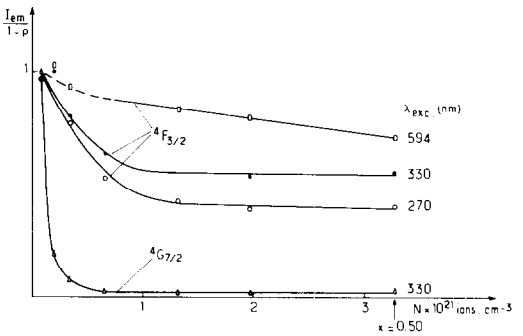

FIG. 4. Variation of the quantum efficiency of the $^4F_{3/2} \rightarrow {}^4I_{9/2}$ and $^4G_{7/2} \rightarrow {}^4I_{11/2}$ emissions versus Nd^{3+} concentration (N) for the $Na_xNd_xCa_{1-2x}Ga_2S_4$ series at 300 K. All curves are normalized at $x = 0.01$ (ρ diffuse reflectance).

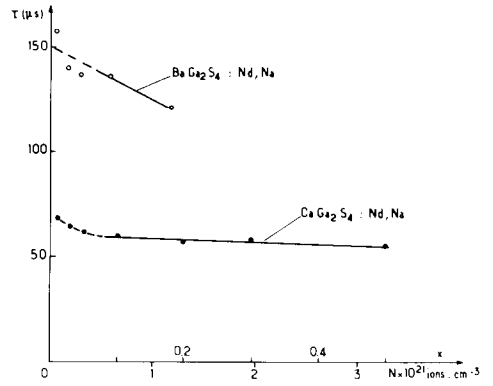

FIG. 5. Concentration dependence of the lifetime of the $^4F_{3/2}$ emission for the $Na_xNd_xM_{1-2x}Ga_2S_4$ phases (M = Ca,Ba) (excitation into the $^2P_{1/2}$ level).

metry which admixes even—and odd—parity wavefunctions (*19*); the decrease in covalency with increasing size of the substituted cation may also contribute to lengthen the lifetime.

Table II shows that despite the high oscillator strengths of the f–f transitions which favor energy transfer, quenching in the $Na_xNd_xCa_{1-2x}Ga_2S_4$ series is smaller than in low-concentration-quenching materials. For the stoichiometric compound, $NaNdGa_4S_8$, the $^4F_{3/2}$ lifetime is only reduced by 1.24. The probability of nonradiative deexcitation by cross-relaxation is considerably reduced when the splitting of the $^4I_{9/2}$ level is lower than 470 cm^{-1} (*15*). The observed value lies well below this limit.

It must be noted that at high neodymium concentrations, the lifetimes are strongly dependent on the excitation rate. The lifetime shortening observed with increasing power of the laser radiation cannot be due to the temperature rise since it also occurs at 80 K. It is probably the result of interactions between excited ions resulting in upconversion (Auger recombination). This process has been observed in NdP_5O_{14} (*16*). Increasing ratio of the $^4G_{7/2}$ to the $^4F_{3/2}$ emission with rising power for excitation at 337 nm supports this assumption. Care was taken of using low excitation rates. Under those conditions, over the time range investigated, beginning 2 μsec after the pulse, no deviation from exponentiality was detected.

II-4. Excitation Spectra

In the case of oxides, over the wavelength range 200–400 nm, the excitation spectra of the neodymium emission contain only weak f–f lines. An intense band whose maximum lies at about 310 nm is present in the spectra of thiogallates (Fig. 6). It shifts slightly to longer wavelengths as the neodymium concentration is increased. Such an intense band has never been reported for neodymium-doped chalcogenides. A weak

TABLE II

CONCENTRATION DEPENDENCE OF THE NEODYMIUM $^4F_{3/2}$ LIFETIMES IN SOME LOW-SELF-QUENCHING MATERIALS

Formula[a]	Maximum Nd concentration (at. $cm^{-3} \times 10^{21}$)	Lifetime (μsec)		τ_0/τ
		At low concentration (τ_0)	At the max. Nd concentration (τ)	
$K_5Li_2Nd_xGd_{1-x}F_{10}$ (*20*)	3.6	510	300	1.7
$LiNd_xLa_{1-x}P_4O_{12}$ (*21*)	4.4	325	135	2.4
$Nd_xLa_{1-x}P_5O_{14}$ (*22*)	4.0	320	120	2.8
$Na_xNd_xCa_{1-2x}Ga_2S_4$	3.23	68	55	1.24

[a] Reference number in parentheses.

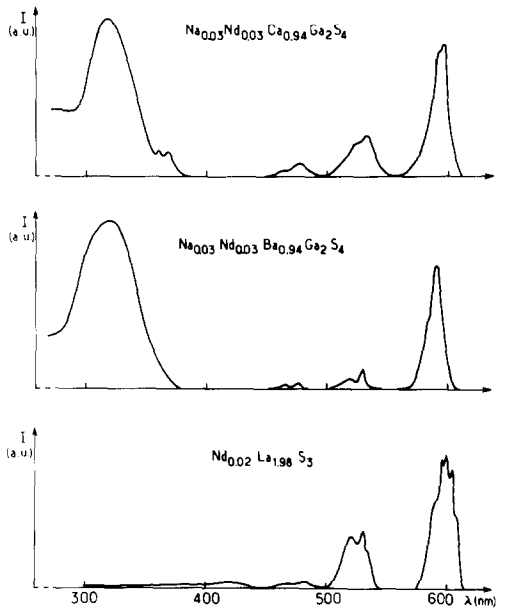

FIG. 6. Excitation spectra of the $^4F_{3/2} \rightarrow {}^4I_{9/2}$ emission of Nd^{3+} in $Na_{0.03}Nd_{0.03}M_{0.94}Ga_2S_4$ (M = Ca, Ba) and La_2S_3:Nd 1% (after Ref. (*7*)).

excitation via the host lattice is observed when Nd^{3+} is incorporated in La_2S_3 (*7*). The previously published spectrum for this material is given in Fig. 6 for comparison. The emission intensity obtained with thiogallates under uv excitation is nearly 2 orders of magnitude more intense.

Reflectance spectra show that the incorporation of neodymium ions brings about an absorption around 310 nm, near the absorption edge of the host lattice (Fig. 7). Comparison with the excitation spectra shows that at low concentration the quantum yield for excitation into this band is comparable to that obtained for excitation into the *f–f* lines.

The band gap of the neodymium sulfides is smaller than that of the gallium sulfides. Therefore, it can be thought that, incorporated at low concentration in the alkaline earth thiogallates, Nd^{3+} forms an impurity level lying below the conduction band. Transfer of an electron from the valence band gives rise to the absorption band around 310 nm. Figure 8 shows that the shape of its low-energy side obtained from the excitation spectra is close to a Gaussian shape as expected at 300 K for transitions followed by strong lattice relaxation (*23*).

The emissions of most of the levels lying above $^4F_{3/2}$ are more intense in $CaGa_2S_4$ than in $BaGa_2S_4$, indicating weaker multiphonon processes. The strong thermal quenching of the highest emitting level, $^4D_{3/2}$ (27,600 cm^{-1}), which occurs between 130 and 230 K may be mainly ascribed to upward transitions to the charge transfer state (CTS). An activation energy of 600 cm^{-1} is derived from the temperature dependence of the intensity, which leads to an energy of about 28,200 cm^{-1} for the CTS in $CaGa_2S_4$.

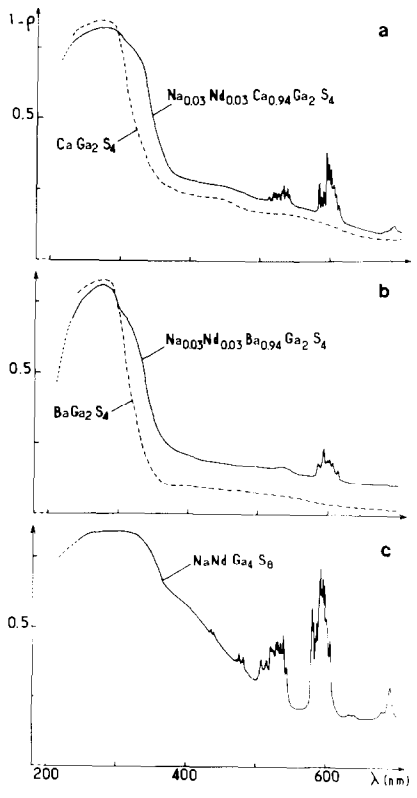

FIG. 7. Diffuse reflectance spectra of thiogallates at 300 K.

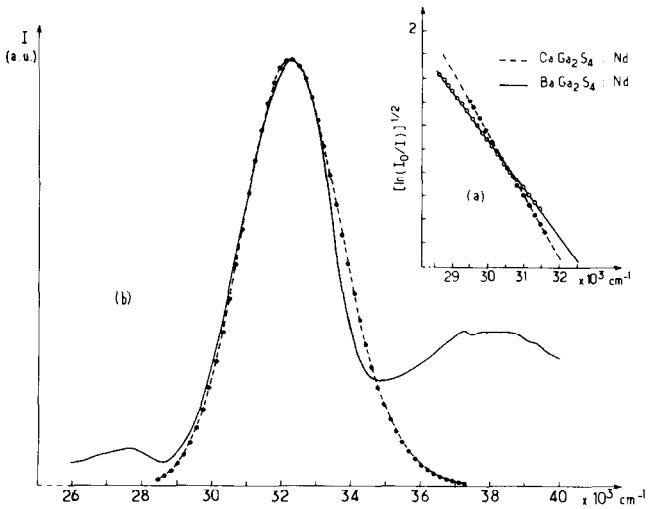

FIG. 8. Investigation of the shape of the charge transfer band. (a) Variation of $[\ln I_0/I]^{1/2} = (1/\sigma)(\tilde{\nu}_0 - \tilde{\nu})$ for the low-energy side not affected by absorption in the host lattice; I_0 and ν_0 are the intensity and the wavenumber at the band maximum. $Na_{0.01}Nd_{0.01}Ca_{0.98}Ga_2S_4$: $\nu_0 = 32{,}150\ cm^{-1}$, $1/\sigma = -5.21 \times 10^{-4}$ cm, $Na_{0.01}Nd_{0.01}Ba_{0.98}Ga_2S_4$: $\nu_0 = 32{,}650\ cm^{-1}$, $1/\sigma = -4.07 \times 10^{-4}$ cm. (b) Comparison of the calculated band shape with experimental data for the calcium phase.

A single-configuration-coordinate diagram was obtained from the shape of the charge transfer band in the excitation spectrum, applying the method proposed by Struck and Fonger (*23*). The u and v representing the parabolae associated with the ground state and the CTS, the rate of a transition between the vibrational states u_n and v_m is considered as proportional to the square overlap $\langle v_m|u_n\rangle^2$ (Franck–Condon factor) and to the normalized Boltzmann weight for the initial state $(1 - r_u)r_u^n$ with $r_u = \exp(-\hbar\omega_u/kT)$ where $\hbar\omega_u$ is the phonon energy for the u state. The m and n levels must be nearly in resonance. An integer quantum number, p_V, that approximates $m - (\hbar\omega_u/\hbar\omega_v)n$ is introduced. The shape of the absorption band is obtained by summing all transitions characterized by the same value of p_V. The $\hbar\omega_u$ was taken equal to 350 cm^{-1}, a value typical of the phonon energies in thiogallates. The configuration coordinate of the minimum of the CTS parabola shows minor variations when $\hbar\omega_u$ is varied from 300 to 400 cm^{-1}. The slope of the straight line $(\ln (I_0/I))^{1/2}$ vs energy (Fig. 8a) and the maximum of the charge transfer band were fitted to the experimental data (Fig. 8b). Figure 9 depicts the configurational diagram so obtained. After lattice relaxation, $4f$ levels associated with parabolae intersecting the CTS curve near its minimum are preferentially populated. It can be seen that losses by transfer to levels lying below $^4F_{3/2}$ are negligible.

With increasing neodymium concentration the absorption band extends to the visible. For $NaNdGa_4S_8$, the increase in absorption starts at about 500 nm (Fig. 7c). Neodymium orbitals likely form the bottom of the conduction band.

Figure 4 shows the concentration dependence of the quantum efficiency of the $^4F_{3/2}$ emission for excitation into the bands made up mainly of Ga levels ($\lambda = 270$ nm) and Nd levels ($\lambda = 330$ nm). The curves reflect both the concentration quenching and the variation of the energy transfer probability to the $4f$ Nd levels. The noticeable initial decrease for excitation at 270 nm may be the

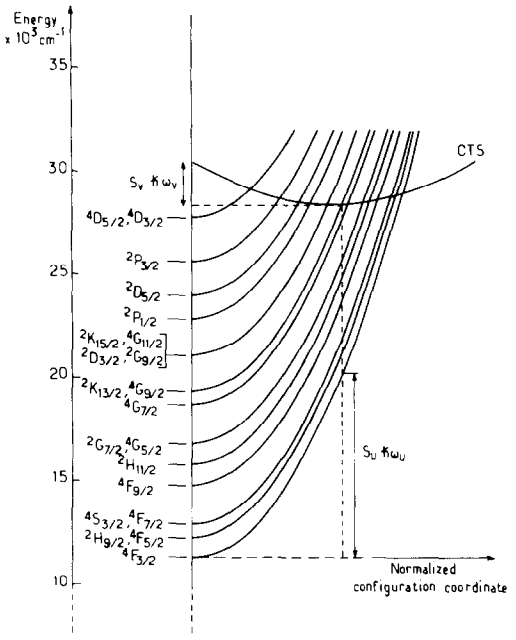

FIG. 9. Single-configuration-coordinate diagram for the Nd^{3+} $4f$ states and the charge transfer state (CTS) in $CaGa_2S_4$ at 295 K (the labels of $4f$ levels correspond to the assignments of Caro *et al.* (*25*)). The best fit to the shape of the charge transfer band leads to $S_u\hbar\omega_u$ = 7900 cm^{-1}, $S_v\hbar\omega_v$ = 2100 cm^{-1}.

result of an increase in the number of defects as the alkaline earth concentration decreases. The simultaneous drop of the curve corresponding to excitation at 330 nm indicates delocalization of the electrons transferred to the neodymium ions. Also in Fig. 4 the curve associated with the $^4G_{7/2}$ emission shows the strong concentration quenching of this level.

III. Conclusion

The $NaNdGa_4S_8$ thiogallate shows two interesting features:

(i) a low concentration quenching which distinguishes this material from sulfides previously investigated and results likely from the presence of neodymium in isolated sites, and (ii) an efficient excitation band.

In sulfides such as ZnS:Nd or La_2S_3:Nd, the conduction band is made up of orbitals belonging to the host: lattice defects which compete with Nd^{3+} ions for capture of charge carriers reduce the transfer efficiency (it can be noted, however, that in a recent paper Scharmer *et al.* have shown that in La_2S_3, transfer from the conduction band to neodymium via Ce^{3+} ions markedly improves the yield (*24*)). The efficient band excitation observed for $NaNdGa_4S_8$ is due to the fact that the bottom of the conduction band is probably constituted essentially by neodymium orbitals. Transfer is also favored by the covalency of the Ga–S bond which limits the number of defects.

References

1. M. R. BROWN AND W. A. SHAND, *J. Mater. Sci.* **5,** 790 (1970).
2. W. W. ANDERSON, S. RAZI, AND D. J. WALSH, *J. Chem. Phys.* **43,** 1153 (1965).
3. W. W. ANDERSON, *J. Chem. Phys.* **44,** 3283 (1966).
4. G. Z. ZHONG AND F. J. BRYANT, *J. Phys. C* **13,** 4797 (1980).
5. G. Z. ZHONG AND F. J. BRYANT, *Solid State Commun.* **39,** 907 (1981).
6. A. KAMINSKII, *Izv. Akad. Nauk SSSR, Neorg. Mater.* **16,** 1333 (1980).
7. M. LEISS, *J. Phys. C* **13,** 151 (1980).
8. R. REISFELD AND A. BORNSTEIN, *Chem. Phys. Lett.* **47,** 194 (1977).
9. F. AUZEL, J. C. MICHEL, J. FLAHAUT, A. M. LOIREAU-LOZAC'H, AND M. GUITTARD, *C.R. Acad. Sci.* **291,** 21 (1980).
10. T. E. PETERS AND J. A. BAGLIO, *J. Electrochem. Soc.* **119,** 230 (1972).
11. A. GARCIA, C. FOUASSIER, AND P. DOUGIER, *J. Electrochem. Soc.* **129,** 2063 (1982).
12. P. C. DONOHUE AND J. E. HANLON, *J. Electrochem. Soc.* **121,** 137 (1974).
13. R. ROQUES, R. RIMET, J. P. DECLERCQ, AND G. GERMAIN, *Acta Crystallogr. Sect. B* **35,** 555 (1979).
14. B. EISENMANN, M. JAKOWSKI, AND H. SCHÄFER, *Mater. Res. Bull.* **17,** 1169 (1982).
15. F. AUZEL, *Mater. Res. Bull.* **14,** 223 (1979).
16. M. BLÄTTE, H. G. DANIELMEYER, AND R. ULRICH, *Appl. Phys.* **1,** 275 (1973).
17. K. OTSUKA, T. YAMADA, M. SARUWATARI, AND T. KIMURA, *IEEE J. Quantum Electron.* **11,** 330 (1975).

18. YU. K. VORON'KO, T. G. MAMEDOV, V. V. OSIKO, A. M. PROKHOROV, V. P. SAKUN, AND I. A. SHCHERBAKOV, *Sov. Phys. JETP* **44,** 251 (1976).

19. H. Y.-P. HONG AND S. R. CHINN, *Mater. Res. Bull.* **11,** 461 (1976).

20. B. C. MCCOLLUM AND A. LEMPICKI, *Mater. Res. Bull.* **13,** 883 (1978).

21. S. R. CHINN, H. Y.-P. HONG, AND J. W. PIERCE, *Laser Focus* **12** (5), 64 (1976).

22. W. LENTH, H. D. HATTENDORF, G. HUBER, AND F. LUTZ, *Appl. Phys.* **17,** 367 (1978).

23. C. W. STRUCK AND W. H. FONGER, *J. Lumin.* **10,** 1 (1975).

24. E.-G. SCHARMER, M. LEISS, AND G. HUBER, *J. Phys. C* **15,** 1071 (1982).

25. P. CARO, D.-R. SVORONOS, E. ANTIC, AND M. QUARTON, *J. Chem. Phys.* **66** (12), 5284 (1977).

26. A. A. KAMARZIN, A. A. MAMEDOV, V. A. SMIRNOV, V. V. SOKOLOV, AND I. A. SHCHERBAKOV, *Sov. J. Quantum Electron.* **13**(3), 328 (1983).